The "Value of Research" Methodology and Hybrid Power Plant Design

Karthik Subramanyan and Urmila M. Diwekar*

Center for Uncertain Systems, Tools for Optimization and Management (CUSTOM) Vishwamitra Research Institute, 34 N. Cass Avenue, Westmont, Illinois 60559

Distributed power generation is one of the most powerful applications of fuel cell power plants. Several types of configurations have been hypothesized and tested for these kinds of applications at the conceptual level, but hybrid power plants are one of the most efficient. These are designs that combine the fuel cell cycle with other thermodynamic cycles to provide higher efficiency. The power plant in focus is the high-pressure (HP)−low-pressure (LP) solid oxide fuel cells (SOFC)/steam turbine (ST)/gas turbine (GT) configuration which is a part of the *Vision-21* program. This program is a new approach that the U.S. Department of Energy's (DOE's) Office of Fossil Energy has begun for developing 21st century energy plants that would have virtually no environmental impact. The overall goal is to effectively eliminate, at competitive costs, environmental concerns associated with the use of fossil fuels for producing electricity and transportation fuels. In this design, coal is gasified in an entrained bed gasifier and the syngas produced is cleaned in a transport bed desulfurizer and passed over to cascaded SOFC modules (at two pressure levels). This module is integrated with a reheat GT cycle. The heat of the exhaust from the GT cycle is used to convert water to steam, which is eventually used in a steam bottoming cycle. Since this hybrid technology is new and futuristic, the system level models used for predicting the fuel cells' performance and for other modules such as the desulfurizer have significant uncertainties in them. Also, the performance curves of the SOFC would differ depending on the materials used for the anode, cathode, and electrolyte. The accurate characterization and quantification of these uncertainties is crucial to the credibility of the model predictions. We have utilized the uncertainty analysis of the (HP−LP)SOFC/ST/GT conceptual design to illustrate the concept of "value of research", which deals with the examination of tradeoffs inherent in allocating scarce resources to reduce uncertainty. Research activities introduce their own costs, and though reducing uncertainty is profitable, the time required to achieve a reduction tempers the benefit and, therefore, needs to be minimized. The "value of research" methodology developed in this work optimizes the objective but, beyond that, limits the extent to which the uncertainty reduction contributes to this goal. The framework developed in this work forms the basis for optimal design and synthesis of any power plant under uncertainties in the face of multiple objectives.

1. Introduction

The "*Vision 21*" (now known as "FutureGen") program is the latest in research efforts undertaken by the U.S. Department of Energy to design power plants with low emissions, high efficiencies, high performance, and low costs. The vision of the program is "to realize sustained domestic economic robustness, enhanced industrial competitiveness and high value jobs creation, while maintaining our respect for our environment, including global climate, and ensuring secure, stable, affordable energy supplies through the creation of clean, efficient, low-cost energy from fossil resources".[1−3] Fuel cells are at the forefront of this program. Their major application is of distributed generation, but a major bottleneck in the design of fuel cell power plants for this application is to package them in a system balance of plant (BoP) that allows them to function effectively. All fuels cells, especially those operating at high temperature, such as molten carbonate fuel cell (MCFC) and solid oxide fuel cell (SOFC), require spent fuel utilization or waste heat recovery subsystems to increase process efficiency. These considerations have fueled the research and development of hybrid power plants where a fuel cell is integrated with other thermodynamic cycles to achieve BoP. Designing such hybrid systems requires integration of several new technologies that are being researched in order to reduce risks and uncertainties. In this paper, we are using a multi-objective optimization framework to address questions important to analyzing research impact, such as how conservative decision makers should be with respect to risks or where limited resources should be allocated in order to reduce uncertainties associated with the new technologies.

A new paradigm called "value of research" is used[4,5] to provide a policy dimension to the traditional optimization problem. The new paradigm is based on a key assumption: that time spent on research increases understanding and, therefore, decreases variation in quantitative estimates derived from this knowledge. Research activities, however, introduce their own costs and risks; hence, time spent learning and experimenting needs to be minimized. While reducing uncertainty is profitable, the time required to achieve a reduction tempers the benefit. The qualitative nature of the value of research objective in contrast to the quantitative benefits of research programs such as the *Vision 21* program (e.g., cost or emission reductions) demands a multi-objective optimization framework. The multi-objective optimization framework provides a set of nondominant decisions where a further improvement for one objective is at the expense of another. This approach finds a set of potentially optimal decisions where tradeoffs can be explicitly identified, unlike cost−benefit analysis, that deals with multiple objectives by identifying a single fundamental objective and then converting all the other objectives into this single currency. Beyond providing a framework in which similar tradeoffs may be

* Corresponding author. Tel.: (630) 515-8772. E-mail: urmila@vri-custom.org.

10.1021/ie0492247 CCC: $33.50
Published on Web 12/21/2005

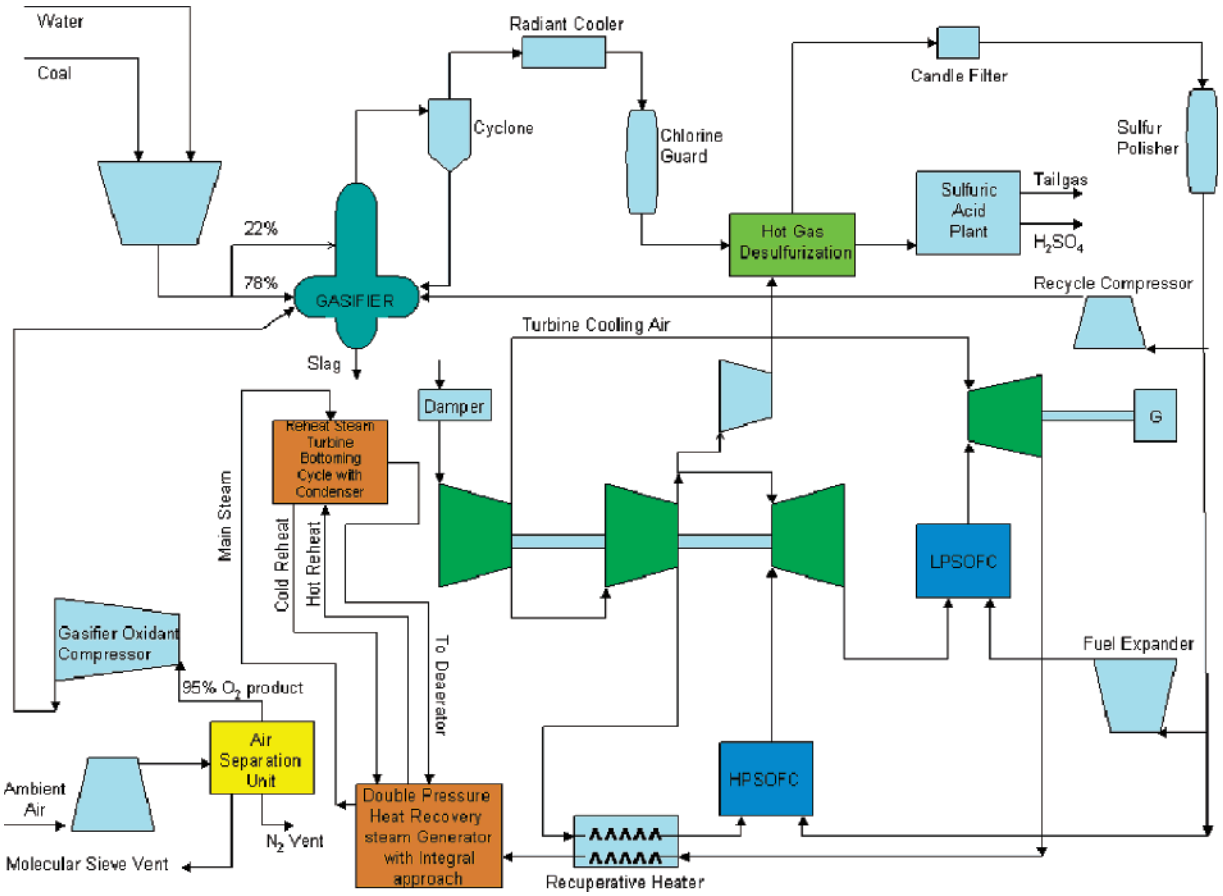

Figure 1. Schematic diagram of the SOFC/ST/GT hybrid power plant.

assessed, the new value of research paradigm also addresses the problem of policy-makers' desire to get answers to specific questions concerning uncertainty. For example, to what extent is imperfect information acceptable, and where should scarce resources be allocated to leverage the impact of these research efforts on the whole of its strategy? Not all sources of uncertainty, after all, are significant.

The value of research framework developed in this paper concerns the high-pressure−low-pressure (HP−LP) solid oxide fuel cell (SOFC)/steam turbine (ST)/gas turbine (GT) hybrid power plant[1] which is a part of the *Vision 21* program. There are multiple objectives: capital cost, CO_2 and SO_2 emissions, HP- and LPSOFC current densities and overall efficiency to be optimized simultaneously.[6] Since this hybrid technology is new and futuristic, the system level models used for predicting the fuel cells' performance and for other modules such as the desulfurizer have significant uncertainties in them. Also, the performance curves of the SOFC would differ depending on the materials used for the anode, cathode, and electrolyte, and analogously, the performance of the desulfurizer module would vary depending on the substance used as the sorbent. These uncertainties are characterized and quantified while the optimization framework is extended to incorporate sampling variance reduction as an attribute for knowledge gained through research. The augmented framework produces results that minimize the objective but, beyond that, limits the extent to which improved understanding contributes to this goal. In this way, the policy dimension of the problem is added to the problem through progressive extensions to the objective functions to include implications of uncertainty.

The section following this introduction gives a brief overview of the SOFC/ST/GT hybrid power plant. Section 3 quantifies and characterizes uncertainties in the important sections of this hybrid power plant. Section 4 describes the "value of information (VoI)" methodology and compares it with the "value of research (VoR)" concept. The section also discusses the theoretical aspects and the mathematical formulation of the VoR methodology with respect to three primary objectives: capital cost, overall efficiency, and SO_2 emissions. Section 5 analyzes some results obtained through this framework, and finally, Section 6 puts forth conclusions derived from this work.

2. Solid Oxide Fuel Cell (SOFC)/Steam Turbine (ST)/Gas Turbine (GT) Hybrid Power Plant Conceptual Design

This section explains the structure of each individual section of the SOFC/ST/GT hybrid power plant briefly. Figure 1 shows the schematic diagram of the power plant and Figure 2 shows the Aspen flowsheet for the *Vision 21* power plant. Only the major blocks have been shown in the flowsheet, and the abbreviation of each section is attached to the respective block names.

2.1. Air Separation Unit (ASU). The purpose of this module is to separate O_2 and N_2 in ambient air since the gasifier requires a pure oxygen stream. Ambient air (O_2 21%, N_2 79%) (AMBAIR) enters the air separation unit (ASU) and is separated into 3 streams: (3) 95% of oxygen to the gasifier, (4) 100% N_2 stream, and (2) remainder to the molecular sieve vent.

2.2. Gasifier Oxidant Compressor (GOC). The oxygen stream from the ASU at ambient conditions is compressed using an isentropic compressor and heated for better gasification performance.

2.3. Coal Preparation (CP). The drycoal is crushed, mixed with water in a hopper resulting in coal slurry with 60 wt % of solids, and passed to the gasifier.

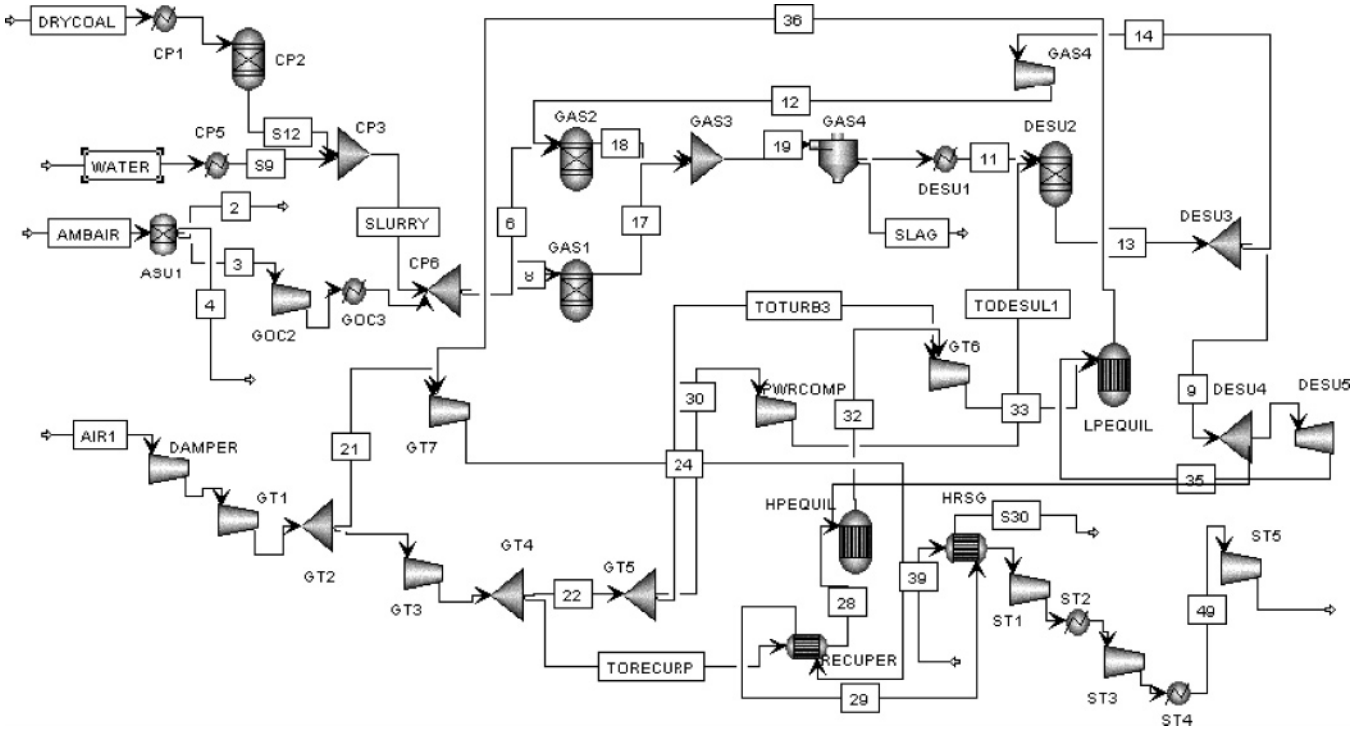

Figure 2. Aspen flowsheet for the *Vision 21* (HP−LP)SOFC/ST/GT hybrid power plant.

2.4. Entrained-Bed Gasifier (GAS). The coal slurry and O_2 streams enter the entrained-bed gasifier. Approximately 78% of the total slurry feed is gasified/combusted in the first (lower) stage (GAS1). Highly exothermic reactions occur that result in temperatures of 2400−2600 °F. In the upper vertical cylindrical stage (GAS2), the remaining coal slurry is fed and additional gasification occurs.

2.5. Desulfurization Module (DESU). The syngas produced during gasification contains prohibitive amounts of H_2S which has to be removed if the plant is to adhere to emission standards. The transport desulfurizer model used in our simulation was based on the work on a hot-gas transport desulfurizer by Luyben and Yi.[7,8] Transport reactors can be operated at a higher gas velocity, which leads to smaller diameter vessels and, hence, lower capital cost. They have the additional advantage of providing better solid/gas contact, so less solid holdup is required.

2.5.1. Brief Overview of the Model. There are assumed to be seven perfectly mixed zones arranged in series in the axial direction. These solid zones have different solid holdups, solids compositions, and temperatures. The gas flows up through these seven zones in series in plug-flow. There are only two phases in the bed: rising gas and solid. Mass transfer and reactions are lumped together by calculating the conversion of H_2S or the production of SO_2 from a reaction rate that assumes first-order dependence on the concentration of the reactant in the gas and the concentration of MeO or MeS in the solid. The reactions that occur in the desulfurizer and regenerator are

$$\text{Sulfidation reaction: } MeO + H_2O \rightarrow MeS + H_2S \quad (1)$$

$$\text{Regeneration reaction: } MeS + 1.5O_2 \rightarrow MeO + SO_2 \quad (2)$$

Because of the small mass of gas in the system, the dynamics of the gas phase are much faster than those of the solid phase. This leads to ordinary differential equations for the gas concentration in each zone with bed height as the independent variable that can be analytically integrated to yield an algebraic equation for the concentration of the gas-phase leaving the top of each of the seven beds at each point in time. The model equations and the schematic diagram are presented in Appendix A. When the model was scaled up to the *Vision 21* hybrid power plant specifications, there were four unknown parameters: (1) mass flow rate of sorbent to the desulfurizer (SRI kg/h), (2) molar flow rate of oxygen to the regenerator (FINRI kg·mol/h), (3) total heat removed from the desulfurizer (QSI kJ/h), and (4) total heat removed from regenerator(QRI kJ/h). These parameters were calculated using an optimization formulation, with minimum H_2S as the objective as shown in Table 1.

Table 1. Optimization Formulation for the Minimization of H_2S

Objective: Minimize "H_2S"
Decision variables:
Vary SRI → bounds: 92000 ≤ SRI ≤110000
Vary FINRI →bounds: 35000 ≤ FINRI ≤ 50000
Vary QSI →bounds: 184400 ≤ QSI ≤ 204000
Vary QRI → bounds: 184400 ≤ QRI≤ 204000
Constraints: 0 ≤ Mole fraction of all components ≤ 1

2.6. High-Pressure and Low-Pressure Solid Oxide Fuel Cells (HP- and LPSOFC). The desulfurized syngas is split and one part is recycled back to the gasifier after compression. The other part is divided between the HP- and LPSOFC, which are at pressures of 15 and 3 atm, respectively. The syngas is expanded before entering the LPSOFC.

2.6.1. Description of an SOFC. The basic physical structure or building block of an SOFC or for any fuel cell consists of an electrolyte layer in contact with a porous anode and cathode on either side. The fuel or oxidant gases flow past the surface of the anode or cathode opposite the electrolyte and generate electrical energy by the electrochemical oxidation of fuel, usually hydrogen, and the electrochemical reduction of the oxidant, usually oxygen. The electrolyte not only transports

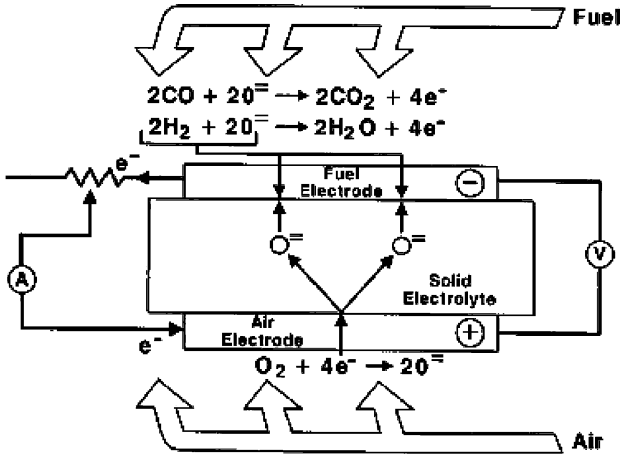

Figure 3. Operating principle of an SOFC.

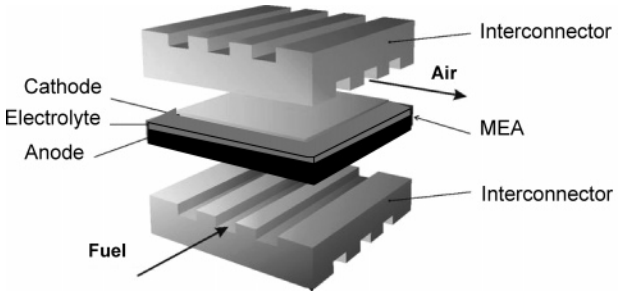

Figure 4. Schematic of an SOFC stack configuration.

dissolved reactants to the electrode but also conducts ionic charge between the electrodes and thereby completes the cell electric circuit. The functions of porous electrodes in fuel cells are to provide a surface site where gas/liquid ionization can take place and to conduct ions away from the interface once they are formed.

Figure 3 shows the operating principle of an SOFC. The electrochemical reactions occurring in an SOFC utilizing H_2 and O_2 are based on eqs 3 and 4.[9]

$$\text{At the anode: } H_2 + O^{=} \rightarrow H_2O + 2e^{-} \tag{3}$$

$$\text{At the cathode: } \frac{1}{2}O_2 + 2e^{-} \rightarrow O^{=} \tag{4}$$

$$\text{Overall cell reaction: } H_2 + \frac{1}{2}O_2 \rightarrow H_2O \tag{5}$$

As with batteries, individual fuel cells must be combined to produce appreciable power levels, and so they are joined in series by interconnects in a stack. Interconnects must be electrical conductors and impermeable to gases. Figure 4 shows a schematic stack configuration of a planar solid oxide fuel cell.

2.6.2. SOFC Models. The SOFC/ST/GT hybrid power plant was modeled using Aspen Plus[10] simulation software, and since the software does not include any inbuilt fuel cell model, two approaches were considered to overcome this problem. The first method was to use a standard reactor model, like a stoichiometric and/or equilibrium reactor, to perform energy and mass balances around the fuel cell. This unit was then to be coupled with a polarization model for voltage and current computations. Alternatively, a new unit (User Model) based on a FORTRAN subroutine could be used to perform mass and energy balances and polarization characterization. The former method was used to model the HPSOFC and LPSOFC modules.

The methodology that was used to simulate the SOFC stack for impact assessment is similar to the one utilized by Geisbrecht.[11] An equilibrium reactor at fixed temperature performs heat and material balances on the cell, and then, after flowsheet convergence, an Aspen calculator block computes voltage, current density, and total cell area by applying a polarization model.

The reactions that take place in a fuel cell are as follows: methane steam reforming, carbon monoxide water shift, and hydrogen electrochemical oxidation.

$$\text{Methane stream reforming: } CH_4 + H_2O \rightarrow 3H_2 + CO \tag{6}$$

$$\text{CO water shift: } CO + H_2O \rightarrow CO_2 + H_2 \tag{7}$$

$$\text{Electrochemical oxidation: } H_2 + \frac{1}{2}O_2 \rightarrow H_2O \tag{8}$$

The first two reactions are at equilibrium,[12] while hydrogen oxidation has a fixed extent in order to match the given fuel utilization. Fuel utilization is defined as

$$U_f = \frac{H_2^{\text{reacted}}}{4CH_4^{\text{in}} + CO^{\text{in}} + H_2^{\text{in}}} \tag{9}$$

where H_2^{reacted} is the total moles of hydrogen reacted and CH_4^{in}, CO^{in}, and H_2^{in} are the moles of methane, carbon monoxide, and hydrogen, respectively, entering the cell. CH_4^{in} is multiplied by 4 in the denominator to represent the number of moles of H_2 generated by each mole of methane and analogously for CO.

The reaction extent of the electrochemical reaction is determined by a "design specification" that acts as a feedback controller. Reaction extent is manipulated so that

$$O_2^{\text{in}} - O_2^{\text{out}} = \frac{1}{2}U_f(4CH_4^{\text{in}} + CO^{\text{in}} + H_2^{\text{in}}) \tag{10}$$

where O_2^{in} and O_2^{out} are the moles of oxygen entering and exiting the cell, respectively, and U_f is the fuel utilization. Oxygen was chosen as the reference element because it reacts only with hydrogen. Recycling of the gaseous outlet of the cell is necessary in order to reach the desired fuel conversion. The electrochemical oxidation of CO was neglected because, in the presence of water, the favorable path for the oxidation of carbon monoxide is the generation of hydrogen by the water shift reaction.[9,12] At a fixed temperature, a heat balance around the reactor gives the power output of the cell. The power output divided by the current (known once the fuel utilization is fixed) gives the voltage of the cell. Current can be computed as

$$I = 2FH_2^{\text{reacted}} = 2FU_f(4CH_4^{\text{in}} + CO^{\text{in}} + H_2^{\text{in}}) \tag{11}$$

where I is the current and F is the Faraday constant (96 485 C/mol). At this point, an SOFC polarization model is used to find the current density of the cell at that given voltage.

There are a number of papers in the literature concerning SOFC polarization modeling. As a first step, they could be classified as steady-state[13−23] and dynamic[24] models. A 1-dimensional, steady-state, algebraic polarization model derived from literature[15] was used for our study. This particular model was chosen because of its simplicity and comprehensive nature (applicability to every operating condition and sensitivity to the various design components of the cell). Overpotential equations, based on the complete Butler−Volmer and diffusion equations,

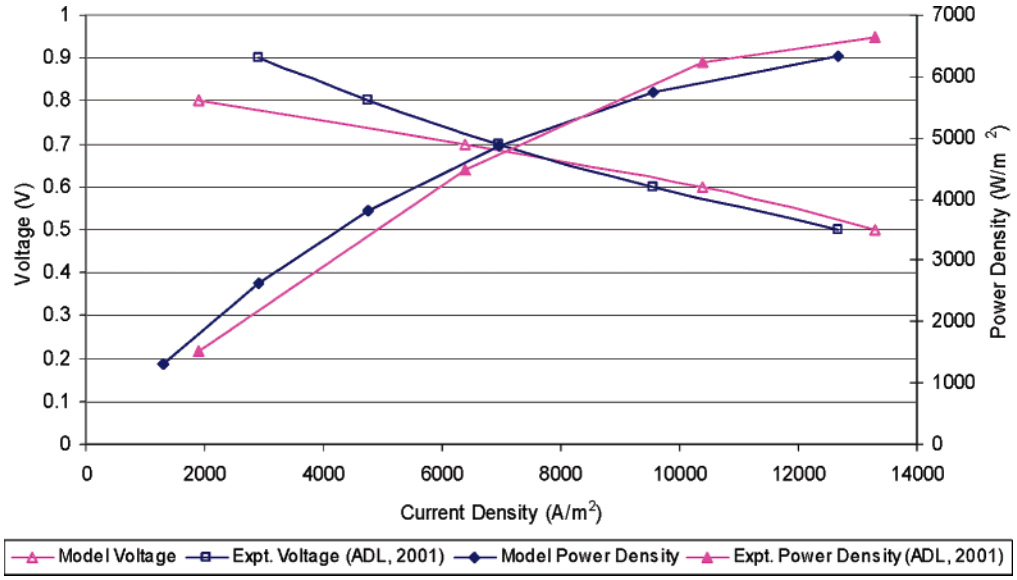

Figure 5. Comparison between model and experimental data.

Table 2. Distribution of Power output between Various Sections of the Power Plant

system performance summary	
gas-turbine cycle power output	133.67 MW
steam-turbine cycle	110.05 MW
HPSOFC	188 MW
LPSOFC	112MW
gross power	560 MW
auxiliary power consumption	40 MW
net power	520 MW

are obtained, together with the necessary parameters from ref 15. The details of this model can be obtained from ref 25.

Since the model gives the voltage as a function of current density, Newton's method was applied in order to iteratively determine the current density at the desired voltage: This polarization model was tested with experimental results from ref 26. Even if the original cell parameters from ref 15 were kept (since no data were provided in ref 26), the fitting between the model and the experimental data was acceptable for our level of detail. The results are shown in Figure 5. Once the current density is obtained, current divided by current density gives the total cell area (area of the electrodes), which isimportant for cost estimations.

2.7. Gas Turbine Cycle (GT). The cascaded HP- and LPSOFC are integrated with the reheat gas turbine cycle, which consists of two air compressors and two expanders. The GT cycle produces a power of ~130 MW

2.8. Steam Turbine Cycle (ST). The heat of the exhaust from the SOFCs is used to convert water to steam in a heat recovery steam generator (HRSG) which is used in a steam bottoming cycle to produces ~118 MW of power.

Table 2 gives the distribution of power output between various sections of the power plant.

3. Uncertainty Characterization and Quantification

The first step in constructing the "value of research" framework is the uncertainty characterization and quantification for the important research areas of the conceptual design. Identification and characterization of uncertainties (knowledge gap) is an important step in our analysis. In reality, the hybrid power plant conceptual design contains numerous uncertain parameters,;however, for the purpose of this paper, we have chosen the parameters which we expect to have the maximum impact on the objectives.

In the hybrid power plant described in Section 2, a large number of materials are needed to be considered in the fuel cells for electrolyte issues, electrode performance issues, and for different configurations, to obtain the desired properties (which leads to uncertainties induced by materials used for the anode−electrolyte−cathode combination). Also, the models developed to simulate the SOFC may not be exact (which leads to uncertainties introduced by model parameters). The performance of the desulfurization module also varies depending on the sorbent used for the absorption. The accurate characterization and quantification of these uncertainties play a crucial role in the proper simulation and accurate prediction of objectives.

In the case of the SOFC current density characteristic, a two-level uncertainty analysis is performed where (1) the uncertainty in the model parameters and (2) the uncertainty induced by the different materials used for anode−electrolyte−cathode combinations are considered. These uncertainties are characterized by a term called the "uncertainty factor (UF)", which is defined as the ratio of the experimental voltage to the model calculated voltage. Taking a particular anode−electrolyte−cathode material combination fuel cell, the UF is computed for all current densities and fit to a probability distribution function. The schematic of this process is given in Figure 6. This process is repeated for all anode−electrolyte−cathode (A−E−C) material combination fuel cells. We had previously performed a literature survey and collected the performance data of 45 A−E−C material combinations.[27] This process resulted in 45 log-normal probability distribution functions for various material combinations with different means and variances characterizing these distributions. The final distribution of all the means together is shown in Figure 7, and Figure 8 shows the distribution for the variance. These two figures present the total uncertainty induced by materials. The UF distribution for a particular material represents the uncertainty associated with purely the model parameters without the "noise" of material uncertainty, and this is shown in Figure 9 for a particular material. In short, the model parameter uncertainty for the SOFC current density characteristic is characterized by log-normal distribution where moments of this distribution are given by material-induced uncertainty distributions.

CeO2-Cu-YSZ / YSZ / YSZ-LSM			
I (A/cm2)	Expt. V	Model V	Uncertainty Factor
0.04	0.96	0.4388	2.187784868
0.08	0.91	0.4303	2.114803625
0.15	0.83	0.4153	1.998555261
0.21	0.76	0.4025	1.888198758
0.31	0.64	0.3814	1.678028317
0.39	0.56	0.3646	1.535929786
0.49	0.46	0.3438	1.337987202
0.56	0.37	0.3293	1.123595506
0.66	0.25	0.3086	0.810110175
0.72	0.21	0.2963	0.708741141
0.81	0.1	0.278	0.35971223
0.86	0.05	0.2678	0.186706497

Uncertainty Factor	PDF
0.1867065	1.90E-02
0.4090486	5.16E-02
0.6313906	0.1738273
0.8537327	0.2997535
1.076075	0.4173072
1.298417	0.5211489
1.520759	0.613921
1.743101	0.6896336
1.965443	0.5753058

Estimated Mean =	1.899683
Estimated Variance =	0.553142

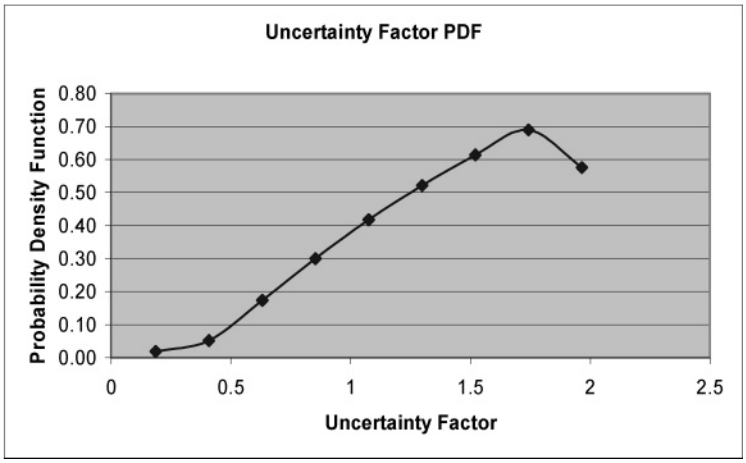

Figure 6. Schematic of the process of uncertainty characterization and quantification for material uncertainty.

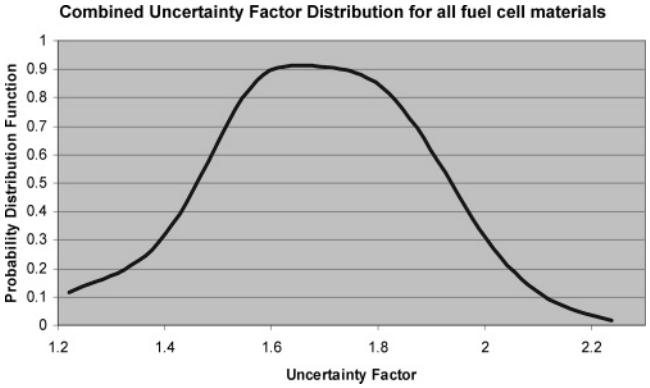

Figure 7. Combined $UF_{mat,mean}$ distribution for fuel cell materials.

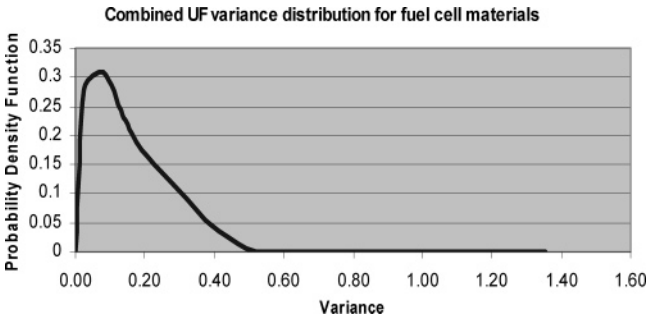

Figure 8. Combined $UF_{mat,var}$ distribution for fuel cell materials.

For the desulfurization module, desulfurization reaction rate constants (k_s) vs temperature (T) Arrhenius plots ($k_s = k_{s0}$ $\exp(-E_a/RT)$) for 20 diferent sorbents generally used in the desulfurization of syngas were collected from the literature. The frequency factor and activation energy data were estimated and fitted into distributions shown in Figures10 and 11, respectively. For a more-detailed explanation and illustration of the uncertainty characterization and quantification process for this hybrid power plant, refer to ref 27. Now the question arises as to how the characterization and quantification of uncertainty is connected to the value of research framework. This is explained in the next section.

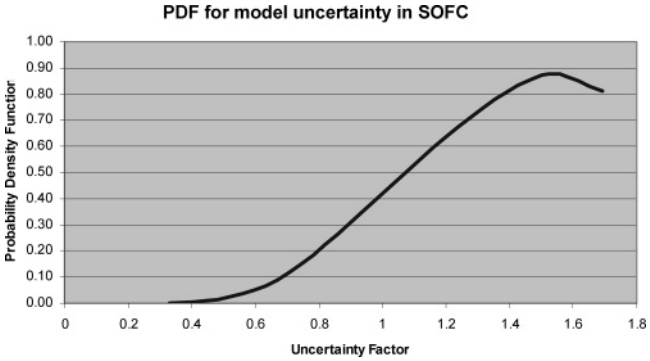

Figure 9. UF_{mod} distribution for uncertainty in fuel cell model parameters.

4. The "Value of Research" Paradigm

The concept of "value of information" (VoI) has been used in the literature to measure the impact of additional data on the primary objective or to calculate the cost of collecting additional

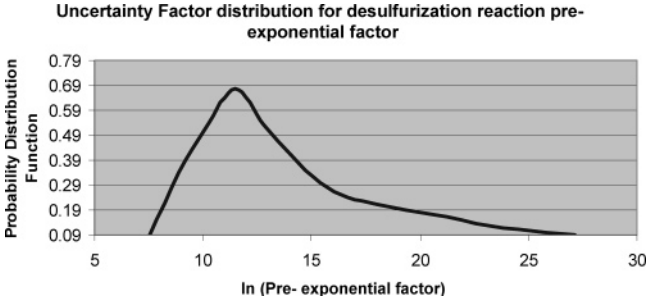

Figure 10. UF distribution for desulfurization reaction preexponential factor.

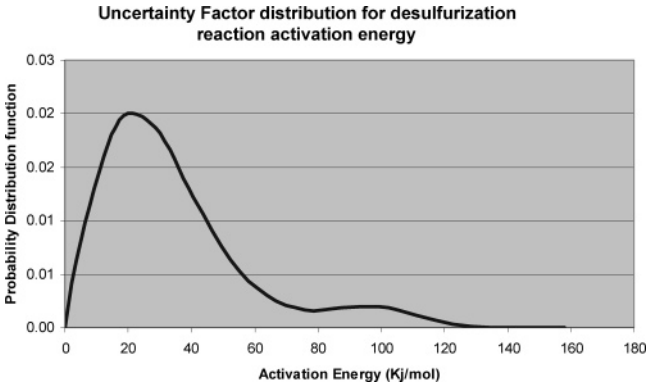

Figure 11. UF distribution for desulfurization reaction activation energy.

data as a measure of knowledge gained by research. In the majority of literature, the value of information was quantified based on economics. For example, Bernardo et al.,[28] while optimizing the cost of a chemical process, calculated the VoI required to reduce the uncertainty of a certain parameter as the sum of a fixed cost (forexample, the cost of a pilot plant for experimentation) and a variable cost (reactant and operation costs) as shown in eq 12.

$$C_{I,j} = b_j C_{\mathrm{If},j} + \alpha_j \left(\frac{1}{\epsilon_j} - \frac{1}{\epsilon_j^{\mathrm{N}}} \right) \tag{12}$$

where $C_{\mathrm{If},j}$ is the fixed cost (forexample, the investment in a pilot plant for experimentation), ϵ_j is the new relative error level in the uncertain parameter θ_j after experimentation, ϵ_j^{N} is the current nominal error level, and b_j is the binary variable that $=0$ if no experiments take place and $=1$ otherwise. Bartell et al.,[29] in their paper concerning VoI in three proposed genetic-screening programs for disease prevention, define VoI as

$$\mathrm{VoI} = \mathrm{TSC}_{\mathrm{baseline}} - \mathrm{TSC}_{\mathrm{option}} \tag{13}$$

where $\mathrm{TSC}_{\mathrm{baseline}}$ is the total social cost for the baseline option (no testing for disease) and $\mathrm{TSC}_{\mathrm{option}}$ is the total social cost for the specified risk management option, defined as

$$\mathrm{TSC} = \mathrm{FC} + r_{\mathrm{p}} B_{\mathrm{d}} \tag{14}$$

where FC is the per capita financial cost of program implementation and B_{d} is the health cost associated with each case of disease.

Diwekar[6] defines the expected value of perfect information (EVPI) as "the difference between the solution obtained when perfect information is available and the optimum solution obtained considering uncertainties". Another method of quantification was the difference between the profits obtained with and without information[30] or the cost incurred to acquire additional information.[31] Meltzer,[32] in his paper dealing with medical cost-effectiveness, defined the cost of information as the increase in "utility" which is a function of medical expenditure, nonmedical consumption, and effectiveness. Similarly Krieger and Hoehn,[33] in their paper on health risk, define "utility" as a function of behavioral choices and states of contamination to health. Ramer and Padet[34] represented VoI as a Shannon entropy function defined as the sum of the product of event frequencies and the logarithm of their reciprocals, which could be considered as a measure of the difficulty of discerning the occurrence of the event. Belief networks and influence diagrams were also used to quantify VoI.[35,36] Other methodologies used were Bayesian Monte Carlo analysis,[37] decision trees,[38] and production digraphs.

In most of these articles, the VoI formulation required data that related funding with error reduction for different stages of the project and was generally defined in terms of cost of information (used only when cost or profit is the objective). In general, VoI analysis provides optimal error levels to be expected for a given funding level.[28] These data are usually not available in research projects, especially those based on new technology like the *Vision 21* hybrid power plants. Further, to calculate VoI, a cost model is required which is also not always available in research projects, and developing one would consume additional resources. In the point-of-view of uncertainties, VoI methodology *does not* establish any sort of relationship between different uncertainties and the objectives. All uncertain parameters are treated on par and are devoted an equal amount of resources. However, it should be remembered that not all sources of uncertainties are significant, and the VoI formulation *does not* provide us a tool to judge the effect of each source of uncertainties on a particular objective so that we understand how to leverage our resources for maximum impact. As stated earlier, VoI formulation is based on an economic objective only. However, in the problem at hand, we have to consider several objectives, such as efficiency, emissions, current density (proxy for reliability and operability), other than just the cost or the profit. Taking all the above factors into consideration, we decided to utilize the concept of "value of research",[4,5] which uses qualitative information to provide knowledge about tradeoffs inherent in allocating scarce resources to alleviate uncertainty sources, not all of which are significant. It is also suitable for multiple objective problems.

4.1. Methodology. The VoR methodology is implemented through additions to the main objective term (e.g., expected capital cost or expected emissions) in the optimization framework. Equation 15 shows a template of this formulation, where we have the main objective plus a term which represents time devoted to reducing uncertainty.

$$\text{Minimize } \{\text{objective and time devoted to reducing uncertainty}\} \tag{15}$$

Here, reduction in uncertainty represented by variance reduction is considered equivalent to gaining more knowledge in order to improve a particular objective. Better characterization of the fuel cell materials or of the model parameters through more research, for instance, would result in a better objective value, for example, a lower capital cost. The decrease in capital cost that a reduction in uncertainty yields, however, must be weighed against the opportunity costs of pursuing the objective. The extensions introduced here facilitate this analysis: an examination of the tradeoffs inherent in allocating scarce resources to

reducing uncertainty. The analysis rests on a key assumption: *that time spent on research* increases understanding and, therefore, decreases variation in quantitative estimates derived from this knowledge. Research activities introduce their own costs and risks; hence, time spent learning and experimenting therefore needs to be minimized. While reducing uncertainty is profitable, the time required to achieve a reduction tempers the benefit.

In the case of the (HP−LP)SOFC/ST/GT hybrid power plant, as mentioned previously, the sampling variance (varsamp) of the uncertainty factor (UF) distribution associated with the fuel cell model and the material and the activation energy and preexponential factor associated with the desulfurization reaction serve as proxies for resources devoted to reducing each uncertainty, respectively. The expanded objective, therefore, attempts to optimize the objective, e.g., capital cost, but, beyond that, limits the extent to which improved uncertain parameter characterization contributes to this goal. Research efforts, for instance, could aim at narrowing the variance of the distribution of the preexponential factor associated with the desulfurization reaction, which would result in better prediction of the extent of H_2S removal, but this process, however, carries an increasing penalty: the time and opportunity costs of related research activities. To understand how the augmented objective captures this tradeoff in mathematical terms, note that the type of investigation relevant to the problem will exhibit diminishing marginal returns as uncertainty declines nonlinearly with time spent on research. For characterization of this phenomenon, an exponential relationship between sampling variance and time provides an adequate first-order functional approximation of this nonlinear dependence:

$$\begin{aligned}&\text{Uncertainty in parameter} <=> \text{varsamp}\\ &\propto \exp(-\text{time}) \text{ or time} \propto -\ln(\text{varsamp})\end{aligned} \tag{16}$$

Once again, minimization of resources devoted to reducing uncertainty is captured in this model by seeking the UF associated with the fuel cell model parameters and materials, the desulfurization reaction activation energy, and the kinetic coefficient with larger input sampling variances. Excessive values, however, are simultaneously penalized through their detrimental effect on the expected capital cost. The optimum reflects a balance in this tradeoff: a low capital cost with moderate values of varsamp.

4.2. "Value of Research" Formulation for the (HP−LP)-SOFC/ST/GT Hybrid Power Plant. For the case of the hybrid power plant, we have implemented the VoR methodology for three primary objectives: capital cost, SO_2 emissions, and overall efficiency. Equations 17, 18, and 19 represent the formulations for the three objectives, respectively. These are extensions of the template shown in eq 15, with the main objective and the sampling variance terms for each of the four uncertain variables. Another point to note here is that, for the purpose of obtaining the full tradeoff surface, the constraint method has better control over the exploration of the nondominated set. However, in general, it has difficulty locating the extreme points.[6] The weighting method, on the other hand, can provide the extreme points easily and is useful in analyzing the relative importance of different solutions. Hence, in this case, we have employed the weighting method, which is used to approximate the nondominated set through the identification of extreme points along the nondominated set.[6]

Minimize

$$\left\{\begin{array}{l}(\text{expected value(capital cost)}) -\\ \quad w1\ln(\sum \text{varsamp}_{\text{model}}) - w2\ln(\sum \text{varsamp}_{\text{material}})\\ -w3\ln(\sum \text{varsamp}_{\text{activation energy}}) -\\ \quad w4\ln(\sum \text{varsamp}_{\text{preexponential factor}})\end{array}\right\}$$

$-\ln(\sum \text{varsamp}_{\text{model}})$ is a proxy for time spent on researching fuel cell models;
$-\ln(\sum \text{varsamp}_{\text{material}})$ is a proxy for time spent on researching fuel cell material; (17)
$-\ln(\sum \text{varsamp}_{\text{preexponential factor}})$ is a proxy for time spent on researching desulfurization reaction preexponential factors for different sorbents;
$-\ln(\sum \text{varsamp}_{\text{activation energy}})$ is a proxy for time spent on researching desulfurization reaction activation energies for different sorbents

Similarly for the minimum SO_2 emissions design, the augmented objective function is

Minimize

$$\left\{\begin{array}{l}\ln(\text{expected value } (SO_2 \text{ emissions})) -\\ \quad w1\ln(\sum \text{varsamp}_{\text{model}}) -\\ w2\ln(\sum \text{varsamp}_{\text{material}})\\ \quad - w3\ln(\sum \text{varsamp}_{\text{activation energy}}) -\\ \quad w4\ln(\sum \text{varsamp}_{\text{preexponential factor}})\end{array}\right\} \tag{18}$$

The exponential log of the objective in this case is for scaling reasons, because the SO_2 emissions is in the order of 10^{-6} mol/kW.

Finally, for the maximum efficiency design, the augmented objective function is

Minimize

$$\left\{\begin{array}{l}-5\ln(\text{expected value (overall efficiency)}) -\\ \quad w1\ln(\sum \text{varsamp}_{\text{model}}) -\\ \quad w2\ln(\sum \text{varsamp}_{\text{material}})\\ -w3\ln(\sum \text{varsamp}_{\text{activation energy}}) -\\ \quad w4\ln(\sum \text{varsamp}_{\text{preexponential factor}})\end{array}\right\} \tag{19}$$

The negative sign is due to the fact that overall efficiency has to be maximized, and it is multiplied by 5 for scaling purposes. The optimization framework illustrated here is *qualitative* in nature. Specific meaning cannot be attached to w_i. The highly nonconvex, nonlinear, and discrete character of the hybrid power plant problem precludes the assessment of "weights" customary to multi-attribute optimization algorithms. The parsimonious choice of an additive objective function, as well as the selection of units and scaling factors for its terms, determines the tradeoffs produced by the variation of w_i. Attention, therefore, should focus not on the w_i term but on the relative changes in the expected values of objectives that adjustments of w_i produce. The w_i are simply a means of assessing tradeoffs between the conflicting goals, in this instance, improving the objective and minimizing the reduction of uncertainty.

The sampling variance for each uncertain parameter was calculated as

$$\text{varsamp}_k = \left(\frac{1}{N}\right)\sum_{i=1}^{N}(x_{i,k} - m_k)^2 \tag{20}$$

where varsamp_k is the sampling variance of the kth uncertain parameter, N is the number of samples of the kth uncertain parameter, $x_{i,k}$ is the ith sample of the kth uncertain parameter, and m_k is the mean of the samples of the kth uncertain parameter.

5. Results and Discussion[39]

Table 3 shows the optimization results for each expected objective optimized individually with the respective w_i combination values. For example, if we consider the second row, the expected capital cost was optimized individually according to the formulation in eq 17 with the w_i parameters as 1,1,1, and 1, respectively. Similarly, in the same row, the expected SO_2 emission was optimized according to the formulation in eq 18 with the same parameter values and analogously for expected overall efficiency. This was repeated for various combinations of w_i, each taking a value of either 1 or 3 (which would mean a relative increase in uncertainty), for each objective, thereby obtaining the data in Table 3. This exercise was performed in order to judge the trend of each objective with increasing emphasis on each uncertain parameter value. The variation in the mean values of a particular objective as the weights for a particular uncertain variable increase from 1 to 3 (meaning that there is an increase in that uncertainty) would gives us an idea of the effect of an increase in the uncertainty of that particular uncertain variable on the particular objective quantitatively. For example, if we take the objective as the expected capital cost and the uncertainty parameter as the model uncertainty, as the weight increases from 1 to 3, the average expected capital cost decreases slightly. In this way, the qualitative effect of an increase in the uncertainty (or minimizing the time devoted to research in that area) was computed. The qualitative results obtained from these data are specified in Table 5. Table 4 gives information on the total variance, taking into consideration all the uncertain variables for each combination of the weights. The average values of decision variables for each objective value in Table 3 resulting from this exercise are given in Table 6.

The reasons for the trends in Table 5 have been analyzed based on the expected decision variable values in Table 6, and the implications of the trends are discussed in the following paragraphs. The results can be used to infer some answers to some important questions in uncertainty analysis—to what extent is imperfect information acceptable, and where should scarce resource be allocated to leverage the impact overall? Not all sources of uncertainty are, after all, significant, and multiobjective optimization works best as an explanatory tool rather than as a means of providing a "one best" solution. The following paragraphs analyze each result individually. These analyses are based on the average decision variable values given in Table 6.

5.1. Minimization of Time Devoted to Material Uncertainty. 5.1.1. Considerable Increase in Overall Efficiency. There are several reasons for this trend. The first reason is that the average inlet mass flowrate of coal has decreased from 219 415.8 lb/h to 211 968.5 lb/h with an increase in uncertainty. Since the power plant has a fixed gross power of 560 MW, this reduction means that the same gross power is produced using a smaller coal rate and, hence, the efficiency has increased. Another reason could be that both the HP- and LPSOFC temperatures have decreased from 1 075.1 and 1 075.37 to 1 044.7 and 1 036.52 °C, respectively. Hence, the auxiliary power consumption to increase their operating temperature from their base case values of 1 000 °C is less. Also, the pressure of the HPSOFC is lower; hence, another auxiliary power component is required to increase the pressure from the base case value of 220 psi. These three factors combine to produce a considerable increase in overall efficiency.

Table 3. Parametric Results of the Trade-off in Reducing Sources of Variation

$w1$	$w2$	$w3$	$w4$	E (capital cost)	E (SO_2 emissions)	E (overall efficiency)
0	0	0	0	2178.4	8.92E−06	0.78
1	1	1	1	2342.47	8.76E−06	0.49
1	3	1	1	2486.44	8.08E−06	0.79
1	1	3	1	2616.89	8.00E−06	0.692
1	1	1	3	2085.12	8.02E−06	0.76
3	1	1	1	2499.05	7.20E−06	0.67
1	3	3	1	2455.75	8.06E−06	0.76
1	1	3	3	2533.43	6.37E−06	0.52
3	1	3	1	2414.04	7.29E−06	0.68
1	3	1	3	2428.48	8.05E−06	0.58
3	1	1	3	2689.7	7.27E−06	0.71
3	3	3	1	2619.84	7.40E−06	0.8
1	3	3	3	2411.97	7.84E−06	0.5
3	1	3	3	2558.85	8.02E−06	0.68
3	3	1	1	2220.95	7.73E−06	0.77
3	3	1	3	2399.21	7.19E−06	0.8
3	3	3	3	2652.21	8.03E−06	0.79

[a] $w1 = \text{varsamp}_{\text{material}}$; $w2 = \text{varsamp}_{\text{model}}$; $w3 = \text{varsamp}_{\text{freq. fac.}}$; and $w4 = \text{varsamp}_{\text{act. ener.}}$.

5.1.2. Considerable Increase in Capital Cost. The first point to note is that the temperature of the HPTEMP has decreased from 952.8 to 902.8 °C and the inlet mass flowrate has decreased from 240 059.3 lb/h to 229 850.2 lb/h (implying a lower amount of syngas produced). Therefore, the HPSOFC net duty in kW (which is directly proportional to both temperature and inlet flowrate) decreased, and the $/kW price of the HPSOFC increased. Also, the average current density of the HPSOFC decreased from 403 to 380 mA/cm^2. Therefore, the area of the fuel cell is increased, thereby increasing the capital cost. Since the net duty of the HPSOFC has decreased and the gross power has been fixed at 560 MW, to maintain this fixed power, the power outputs of the steam turbine and gas turbine have to increase and their costs, which are directly proportional to the amount of power they produce as shown in eqs 24 and 25, are also increased.

$$\text{Gas turbine cycle cost: } 185\text{MW}_{\text{GT}} + 0.07 \times 185\text{MW}_{\text{GT}} \tag{21}$$

where MW_{GT} is the electrical output of the gas turbine section in megawatts.

$$\text{Steam turbine cost: } 158\text{MW}_{\text{ST}} \tag{22}$$

where MW_{ST} is the electrical output of the steam turbine section in megawatts.

5.1.3. Considerable Decrease in SO_2 Emissions. The SO_2 emission objective is most sensitive to the temperature of syngas entering the desulfurizer module (TRADC). Note that the TRADC has decreased by ~130 °C. The temperatures of the seven zones in the desulfurizer and of the regenerator are also decreased due to a decrease in the inlet gas temperature. The amount of SO_2 produced in the regenerator is dependent on the temperature of the regenerator. Hence, the amount of SO_2 production is decreased. Another scenario is that the lower inlet temperature implies a lower conversion value for the desulfurization reaction. Hence, there would be less spent sorbent and

Table 4. Variance of the Uncertainty Parameters for Each Parametric Combination

$w1$	$w2$	$w3$	$w4$	material	model	frequency factor (FF)	activation energy (AE)	total ($w1 \times$ mat + $w2 \times$ mod + $w3 \times$ FF + $w4 \times$ FF)
0	0	0	0	0.000 295	0.031 486	8.297 02	203.453 1	0
1	1	1	1	0.000 295	0.031 486	8.297 02	203.453 1	211.781 901
1	3	1	1	0.000 295	0.094 458	8.297 02	203.453 1	211.844 873
1	1	3	1	0.000 295	0.031 486	24.891 06	203.453 1	228.375 941
1	1	1	3	0.000 295	0.031 486	8.297 02	610.359 3	618.688 101
3	1	1	1	0.000 885	0.031 486	8.297 02	203.453 1	211.782 491
1	3	3	1	0.000 295	0.094 458	24.891 06	203.453 1	228.438 913
1	1	3	3	0.000 295	0.031 486	24.891 06	610.359 3	635.282 141
3	1	3	1	0.000 885	0.031 486	24.891 06	203.453 1	228.376 531
1	3	1	3	0.000 295	0.094 458	8.297 02	610.359 3	618.751 073
3	1	1	3	0.000 885	0.031 486	8.297 02	610.359 3	618.688 691
3	3	3	1	0.000 885	0.094 458	24.891 06	203.453 1	228.439 503
1	3	3	3	0.000 295	0.094 458	24.891 06	610.359 3	635.345 113
3	1	3	3	0.000 885	0.031 486	24.891 06	610.359 3	635.282 731
3	3	1	1	0.000 885	0.094 458	8.297 02	203.453 1	211.845 463
3	3	1	3	0.000 885	0.094 458	8.297 02	610.359 3	618.751 663
3	3	3	3	0.000 885	0.094 458	24.891 06	610.359 3	635.345 703

Table 5. Qualitative Summary of the Trade-off in Reducing Sources of Variation

focus of research	E (capital cost)	E (SO_2 emissions)	E (overall efficiency)
minimize time devoted to fuel cell material research	considerable increase	considerable decrease	considerable increases
minimize time devoted to fuel cell model research	slight decrease	moderate increase	considerable increase
minimize time devoted to preexponential factor research	considerable increase	moderate decrease	slight decrease
minimize time devoted to activation energy research	slight increase	moderate decrease	moderate decrease

Table 6. Values of Average Decision Variables for Each Uncertain Parameter

	capital cost		SO_2 emissions		overall efficiency	
	$w_i = 1$	$w_i = 3$	$w_i = 1$	$w_i = 3$	$w_i = 1$	$w_i = 3$
			materials uncertainty			
HPTEMP (°C)	952.85832	902.8263	1104.981	1046.666	1075.103	1044.787
LPTEMP (°C)	1080.314446	1104.244	1015.216	1005.673	1073.375	1036.525
RATIO	0.432114524	0.405554	0.514331	0.48437	0.514951	0.437299
FUT	0.530378353	0.548405	0.548894	0.628902	0.599305	0.554235
HPPRES (psi)	414.2207135	448.5163	317.1282	287.7943	479.9146	387.5859
DRYCOA (lb/h)	240059.3412	229850.2	218459.1	236776.2	219415.8	211968.5
TRADC (°C)	939.8744877	562.1499	883.2505	755.7098	698.5237	748.7099
			model uncertainty			
HPTEMP (°C)	929.8061083	925.8785	1060.05	1091.596	1049.108	1070.782
LPTEMP (°C)	1095.962801	1088.595	994.7315	1026.157	1046.295	1063.604
RATIO	0.425654263	0.412014	0.493253	0.505448	0.483462	0.468788
FUT	0.497935912	0.580847	0.607964	0.569833	0.5942	0.55934
HPPRES (psi)	459.6290708	403.108	271.6585	333.2641	365.6303	501.8702
DRYCOA (lb/h)	221264.1749	248645.4	216583.9	238651.5	229378.7	202005.5
TRADC (°C)	778.584395	723.44	848.1531	790.8073	769.6368	677.5967
			frequency factor uncertainty			
HPTEMP (°C)	920.6801096	935.0045	1084.197	1067.449	1012.003	1107.887
LPTEMP (°C)	1087.738233	1096.82	1027.093	993.7963	1076.967	1032.933
RATIO	0.423539396	0.414129	0.538889	0.459812	0.490664	0.461586
FUT	0.533241249	0.545542	0.641978	0.535818	0.647874	0.505666
HPPRES (psi)	400.6243727	462.1127	333.9305	270.992	451.2139	416.2866
DRYCOA (lb/h)	239354.833	239554.7	218370.3	236865.1	217900.3	213483.9
TRADC (°C)	848.1294303	653.8949	900.9891	737.9713	744.8423	702.3913
			activation energy uncertainty			
HPTEMP (°C)	912.5651053	943.1195	1084.07	1067.576	1074.774	1045.116
LPTEMP (°C)	1084.028576	1100.53	1026.691	994.1982	1054.534	1055.365
RATIO	0.435559018	0.402109	0.538191	0.460509	0.469179	0.483071
FUT	0.551345456	0.527438	0.641939	0.535857	0.585407	0.568133
HPPRES (psi)	432.354549	430.3825	332.7663	272.1562	444.2088	423.2916
DRYCOA (lb/h)	229042.2122	240867.3	217838.8	237396.5	215823.8	215560.4
TRADC (°C)	804.959576	697.0648	900.0346	738.9257	748.3782	698.8554

less SO_2 production. Another reason could be that the fuel utilization in this case has increased from 0.54 to 0.63. Therefore, more hydrogen reacts with more oxygen in the SOFC, which means that, in the recycle stream from the SOFCs to the desulfurizer (which is a lower amount of O_2 in the regenerator to react with the metal sulfide to form SO_2. Since the driving force for the regeneration reaction is lower, the production of SO_2 decreased. These two factors combine to produce a considerable decrease in SO_2 emissions.

5.2. Minimization of Time Devoted to Fuel Cell Model Uncertainty. 5.2.1. Considerable Increase in Overall Efficiency. The major reason is that, again, the plant is of a fixed power of 560 MW. The inlet mass flowrate has significantly decreased from 229 378.7 to 202 005.5 lb/h, and so the same power is produced by considerably less coal and the efficiency has increased significantly. Also, the TRADC has decreased by ~100 °C, and so the auxiliary consumption has decreased.

5.2.2. Slight Decrease in Capital Cost. Note that the inlet drycoal mass flowrate has increased moderately and, hence, sections such as coal handling and gasification which depend on this rate will experience a moderate increase in capital cost. But also, the fuel utilization has increased from 0.49 to 0.58, which means better performance of the fuel cell per unit area and, hence, the cost of the fuel cell has decreased. These two factors compensate each other, and the overall result is a slight decrease in the capital cost.

5.2.3. Moderate Increase in SO_2 Emissions. The TRADC has decreased moderately by ~50 °C. This implies moderately lower SO_2 production for similar reasons to those mentioned above. But at the same time, the inlet mass flowrate has increased from 216 573.9 to 238 651.5 lb/h. So, this implies more syngas production and, hence, more H_2S. More H_2S means the driving force for the desulfurization reaction has increased. This leads to more spent sorbent and, hence, an increased SO_2 production. Moreover, the fuel utilization has varied only slightly, meaning it does not have much impact on SO_2 emission. The overall result is, therefore, a moderate increase in the SO_2 production.

5.3. Minimization of Time Devoted to Frequency Factor Uncertainty. 5.3.1. Considerable Increase in Capital Cost. The average current density of the HPSOFC remains more or less constant, but that of the LPSOFC decreases from 429.74 to 384.21 mA/cm^2. As mentioned before, this results in an increased fuel cell area and, thereby, an increased capital cost.

5.3.2. Slight Decrease in Overall Efficiency. In this case, the difference between the coal inlet mass flow rates is more or less similar. Also, the HPTEMP has increased while the LPTEMP has decreased, and the changes in HPPRES and TRADC are not considerable, so the change in auxiliary power consumption is small. The overall effect is that the efficiency decreases slightly but not much.

5.3.3. Moderate Decrease in SO_2 Emissions. The TRADC has decreased moderately by ~50 °C. This implies moderately lower SO_2 production for similar reasons to those mentioned above. Another factor which causes the increase in SO_2 production is the increase in the inlet mass flowrate of drycoal, leading to an increase in H_2S, which increases the driving force for desulfurization, leading to more spent sorbent and more SO_2 production. Finally, the overall effect is a moderate decrease in SO_2 emission.

5.4. Minimization of Time Devoted to Activation Energy Uncertainty. 5.4.1. Slight Increase in Capital Cost. Note that the inlet drycoal mass flowrate has increased moderately, and hence, sections such as coal handling and gasification which depend on this rate will experience a moderate increase in capital cost. But at the same time, the current densties of HP- and LPSOFC have increased from 369.04 and 360 mA/cm^2 to 415 and 453.3 mA/cm^2. This results in a lesser area for both the SOFCs, leading to a lower capital cost. These two effects compensate each other, and the overall impact is a slight increase in the capital cost.

5.4.2. Moderate Decrease in SO_2 Emissions. The reasons for a moderate decrease in SO_2 emissions would be the same as those mentioned for the preexponential factor case, because the trends in decision variables are similar.

5.4.3. Moderate Decrease in the Overall Efficiency. The values of the decision variables in this case do not give a clear reason for this trend. This can be attributed, like other trends, to the high nonlinearity of the model.

5.5. Some Qualitative Inferences from the Results. The importance of devoting more resources for desulfurization reaction research is apparent in Table 5. The results in this case are intuitive, i.e., as anticipated, the expected capital cost increases qualitatively as the time devoted to the research on the two uncertain parameters pertaining to the desulfurization reaction, preexponential factor and activation energy, are minimized. But the quantitative increase is much higher for the preexponential factor uncertainty compared to that for the activation energy, where there is only a slight increase. So for practical purposes, it can be inferred that activation energy uncertainty does not have an impact on the capital cost. The expected overall efficiency decreases moderately with an increase in activation energy uncertainty and remains more or less constant with preexponential factor uncertainty. So overall, the desulfurization reaction uncertainty has a negative impact on the capital cost and overall efficiency. Hence, it is advisable to allocate more resources for desulfurization reaction research. One interesting fact to note is that the expected SO_2 emissions decrease (more in the case of activation energy uncertainty) with increases in both of these uncertainties, and in this case, imperfect information seems to be acceptable to a certain extent. This compromise illustrates the balance between decreasing the SO_2 emissions but compromising on the capital cost and overall efficiency when resources are not allocated for desulfurization reaction research. It is up to the decision maker to decide whether he/she wants to spend more resources on reducing these uncertainties, and the decision could be based on the emission standards in the geographical region.

If the plant is located in a geographical region where the emission standards are very stringent, it would be preferable to spend more resources on fuel cell model uncertainty, because it is seen from Table 5 that the SO_2 emissions increase with an increase in this uncertainty. Also, there is only a minor variation in the capital cost with an increase in this uncertainty. Hence again, for practical purposes, it can be inferred that the fuel cell model uncertainty does not have an impact on the capital cost. Also in this case, imperfect information seems to be acceptable to a considerable extent, since overall efficiency has not been affected adversely by an increase in this uncertainty. The fuel cell material uncertainty has a significant impact on the capital cost, since this objective increases appreciably when time devoted on its research is minimized. On the other hand, the SO_2 emissions and overall efficiency have not been affected adversely, and also for this uncertainty, impact on one objective can be compensated by trading-off with other objectives, which is not possible in the case of the desulfurization reaction uncertainty. Hence, the fuel cell material uncertainty comes only after the desulfurization uncertainty as the area for allocation of more resources for uncertainty reduction, while fuel cell model uncertainty comes last. Ultimately, it all depends on the decision maker's priority. If he/she holds paramount importance to the SO_2 emission objective, the fuel cell model uncertainty would gain priority over the others because it has the maximum impact on the objective. Following the same argument, if the overall efficiency is the most important objective to the decision maker, then desulfurization reaction uncertainty reduction would gain priority. Finally, if the capital cost were the most significant, the fuel cell material and desulfurization preexponential factor would be pre-eminent. Hence, the "value of research" methodology can only predict the qualitative trends of the objectives based on allocation of resources for uncertainty minimization, but it is solely up to the decision maker to prioritize his objectives and leverage the available resources effectively.

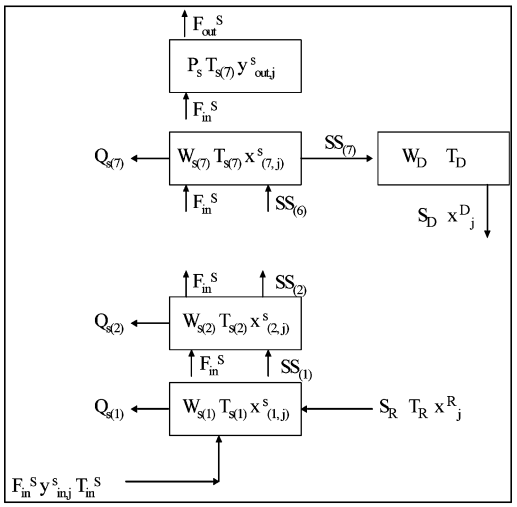

Nomenclature:

$Q_{s(i)}$: Heat removed from ith zone in desulfurizer (Kj/hr);
T^s_{in} : Temp.of inlet syn-gas to desulf. (deg.C)
$y^s_{in,j}$: mole fr. of jth component in inlet gas to desulf;
F^s_{in} : Mole flow of inlet syn-gas to desulf (kgmol/hr)
$W_{s(i)}$: solids hold-up in ith zone in desulf. (kg);
F^s_{out} : Mole flow of outlet syn-gas from desulf (kgmol/hr)
$T_{s(i)}$: Temp. of ith zone in desulf. (°C);
$y^s_{out,j}$: mole fr. of jth component in inlet gas to desulf;
$x^s_{i,j}$:mole fr. of jth component of solid in ith zone in desulf;
W_D : solids hold-up in drum (kg)
SS_i : solid flowrate from ith zone in desulf (kg/hr);
x^D_j : mole fr. of jth component of solid in drum
T_D : Temp. in drum (°C);
S_R : Solids flowrate from regen. to desulf. (kg/hr)
S_D : solid flow rate from drum (kg/hr);
T_R : Temp. in regenerator (°C);
x^D_j : mole fr. of jth component of solid in regenerator

Figure 12. Schematic of the desulfurizer model used in the SOFC/ST/GT simulation.

6. Conclusions

This paper presented a framework to evaluate the trade offs between allocation of resources to alleviate the uncertainty in a certain parameter and the benefits accrued to the objectives through this reduction. The framework attempted to answer policy-oriented questions such as the following: What is the value of doing more research? How much time and resources should be allocated for conducting more research to reduce uncertainties? Are the benefits worth the cost?

As a first step in answering these questions, a literature survey on the concept of "value of information" was performed and, from the collected data, it was concluded that "value of research (VoR)" was the more suitable methodology for our case. A VoR framework was constructed through an augmented objective function based on the weighted method. The trends for each objective based on the uncertainty reduction were obtained. The average decision variable values were used to explain the reasons for these trends. Some of the inferences derived from the trends were that uncertainty in materials had the most profound effect on the objectives, though not always negative. The capital cost was affected negatively, while the SO_2 emissions and overall efficiency were not; also for this uncertainty, the impact on one objective could be compensated by trading-off with other objectives. The desulfurization reaction uncertainty had two components: frequency factor and activation energy uncertainties. Overall, this uncertainty adversely affected the SO_2 emission moderately, and in particular, the frequency factor uncertainty affected the capital cost substantially. The fuel cell model uncertainty had the least impact on the objectives overall, but it had a moderate negative impact on SO_2 emissions and affected the overall efficiency positively. Hence, finally, the conclusion was that desulfurization reaction uncertainty had the highest priority for allocation of resources, next came fuel cell material uncertainty, and last was fuel cell model uncertainty. These trends give an idea to the decision maker about which uncertainties are important and where to leverage his/her resources for maximum impact. The final allocation of resources would be based, apart from these trends, on the decision maker's priority of objectives.

Acknowledgment

The funding for this work is provided by NETL/DOE, Morgantown, WV, and thanks is given to Francesco Baratto for the SOFC model code.

Appendix A: Equations for the Desulfurization/ Regenerator Mode[7,8]

A schematic of the desulfurizer model is given in Figure 12.

Desulfurizer Equations.

Gas-phase mass balance (kg/h)

$$\frac{\mathrm{d}(V^{\mathrm{S}}_{\mathrm{G}}\rho^{\mathrm{S}}_{\mathrm{G}})}{\mathrm{d}t} = F^{\mathrm{S}}_{\mathrm{in}}M^{\mathrm{S}}_{\mathrm{in}} - F^{\mathrm{S}}_{\mathrm{out}}M^{\mathrm{S}}_{\mathrm{out}} - (34.08 - 18.02)\sum_{k=1}^{7}R_{\mathrm{H_2S},k} \quad \text{(A1)}$$

Gas-phase component balances

(kg·mol h^{-1} of component j) for $j = \mathrm{H_2}$, $\mathrm{CO_2}$, CO

$$\frac{\mathrm{d}\left(\dfrac{V^{\mathrm{S}}_{\mathrm{G}}\rho^{\mathrm{S}}_{\mathrm{G}}y^{\mathrm{S}}_{\mathrm{out},j}}{M^{\mathrm{S}}_{\mathrm{out}}}\right)}{\mathrm{d}t} = F^{\mathrm{S}}_{\mathrm{in}}y^{\mathrm{S}}_{\mathrm{in},j} - F^{\mathrm{S}}_{\mathrm{out}}y^{\mathrm{S}}_{\mathrm{out},j} \quad \text{(A2)}$$

Gas-phase component balances

(kg·mol h^{-1} of component j) for $j = \mathrm{H_2S}$

$$\frac{\mathrm{d}\left(\dfrac{V^{\mathrm{S}}_{\mathrm{G}}\rho^{\mathrm{S}}_{\mathrm{G}}y^{\mathrm{S}}_{\mathrm{out},j}}{M_{\mathrm{out}}{}^{\mathrm{S}}}\right)}{\mathrm{d}t} = F^{\mathrm{S}}_{\mathrm{in}}y^{\mathrm{S}}_{\mathrm{in},j} - F^{\mathrm{S}}_{\mathrm{out}}y^{\mathrm{S}}_{\mathrm{out},j} - \sum_{k=1}^{7}R_{\mathrm{H_2S},k} \quad \text{(A3)}$$

Gas-phase component balances

(kg·mol h^{-1} of component j) for $j = \mathrm{H_2O}$

$$\frac{\mathrm{d}\left(\dfrac{V^{\mathrm{S}}_{\mathrm{G}}\rho^{\mathrm{S}}_{\mathrm{G}}y^{\mathrm{S}}_{\mathrm{out},j}}{M^{\mathrm{S}}_{\mathrm{out}}}\right)}{\mathrm{d}t} = F^{\mathrm{S}}_{\mathrm{in}}y^{\mathrm{S}}_{\mathrm{in},j} - F^{\mathrm{S}}_{\mathrm{out}}y^{\mathrm{S}}_{\mathrm{out},j} + \sum_{k=1}^{7}R_{\mathrm{H_2S},k} \quad \text{(A4)}$$

Gas density (kg/m^3)

$$\rho_G^S = \frac{M_{out}^S P_S}{0.082\,057(T_{S,7} + 273)} \quad \text{(A5)}$$

Solid-phase mass balance for kth zone (kg/h)

$$\frac{dW_{S,k}}{dt} = SS_{k-1} - SS_k + (32 - 16)R_{H_2S,k} \quad \text{(A6)}$$

Solid-phase component balance for kth zone (kg/h)

(kg/h of component j = MeO)

$$\frac{d(W_{S,k}x_{k,j}^S)}{dt} = SS_{k-1}x_{k-1,j}^S - SS_k x_{k,j}^S - 81.4R_{H_2S,k} \quad \text{(A7)}$$

Solid-phase component balance for kth zone (kg/h)

(kg/h of component j = MeS)

$$\frac{d(W_{S,k}x_{k,j}^S)}{dt} = SS_{k-1}x_{k-1,j}^S - SS_k x_{k,j}^S + 97.4R_{H_2S,k} \quad \text{(A8)}$$

Solid-phase component balance for kth zone (kg/h)

(kg/h of component j = inert)

$$\frac{d(W_{S,k}x_{k,j}^S)}{dt} = SS_{k-1}x_{k-1,j}^S - SS_k x_{k,j}^S \quad \text{(A9)}$$

Solid-phase energy balance for kth zone (kJ/h)

$$\frac{d(0.322W_{S,k}T_{S,k})}{dt} = 0.322(SS_{k-1}T_{S,k-1} - SS_k T_{S,k}) + 36F_{in}^S(T_{S,k-1} - T_{S,k}) - Q_{S,k} \quad \text{(A10)}$$

Solid-phase energy balance for 1st zone (kJ/h)

$$\frac{d(0.322W_{S,1}T_{S,1})}{dt} = 0.322(SS_R T_R - SS_1 T_{S,1}) + 36(F_{in}^S T_{in}^S - F_{out}^S T_{S,1}) - Q_{S,1} \quad \text{(A11)}$$

Solids flow rate from kth zone (kg/h)

$$SS_k = SS_{k-1} + K_{flow,k}(W_{S,k} - W_{S,k-1}) \quad \text{(A12)}$$

Kinetics for kth zone

$$-R_{H_2O,k} = R_{H_2S,k} = Conv_{S,k}^{actual} F_{in}^S y_{k,H_2S}^S \quad \text{(A13)}$$

$$Conv_{S,k}^{ideal} = 1 - \exp\left(-\frac{W_{S,k}K_{S,k}x_{k,MeO}^S}{F_{in}^S}\right) \quad \text{(A14)}$$

where

$$K_{S,k} = (\text{factor})7.694 \times 10^6 \exp\left(-\frac{7\,240}{T_{S,k} + 273}\right) \quad \text{(A15)}$$

$$Conv_{S,k}^{actual} = (\text{Eff})Conv_{S,k}^{ideal} \quad \text{(A16)}$$

Gas compositions leaving kth zone

$$y_{k,H_2S}^S = y_{k-1,H_2S}^S(1 - Conv_{S,k}^{actual}) \quad \text{(A17)}$$

$$y_{k,H_2O}^S = y_{k-1,H_2O}^S + y_{k-1,H_2S}^S Conv_{S,k}^{actual} \quad \text{(A18)}$$

Regenerator Equations.

Gas-phase mass balance (kg/h)

$$\frac{d(V_G^R\rho_G^R)}{dt} = F_{in}^R M_{in}^R - F_{out}^R M_{out}^R - M_{O_2}R_{O_2} + M_{SO_2}(2/3)R_{O_2} \quad \text{(A19)}$$

Gas-phase component balances

(kg·mol h^{-1} of component j) for $j = N_2$

$$\frac{d\left(\frac{V_G^R\rho_G^R y_{out,j}^R}{M_{out}^R}\right)}{dt} = F_{in}^R y_{in,j}^R - F_{out}^R y_{out,j}^R \quad \text{(A20)}$$

Gas-phase component balances

(kg·mol h^{-1} of component j) for $j = O_2$

$$\frac{d\left(\frac{V_G^R\rho_G^R y_{out,j}^R}{M_{out}^R}\right)}{dt} = F_{in}^R y_{in,j}^R - F_{out}^R y_{out,j}^R - R_{O_2} \quad \text{(A21)}$$

Gas-phase component balances

(kg·mol h^{-1} of component j) for $j = SO_2$

$$\frac{d\left(\frac{V_G^R\rho_G^R y_{out,j}^R}{M_{out}^R}\right)}{dt} = FF_{in}^R y_{in,j}^R - F_{out}^R y_{out,j}^R - R_{SO_2} \quad \text{(A22)}$$

Gas density (kg/m^3)

$$\rho_G^R = \frac{M_{out}^R PR}{0.082\,057(T_R + 273)} \quad \text{(A23)}$$

Solid-phase mass balance (kg/h)

$$\frac{dW_R}{dt} = S_S - S_R - (M_{MeS} - M_{MeO})(2/3)R_{O_2} \quad \text{(A24)}$$

Solid-phase component balance (kg/h)

(kg/h of component k = MeO)

$$\frac{d(W_R x_k^R)}{dt} = S_S x_k^S - S_R x_k^R + M_{MeO}(2/3)R_{O_2} \quad \text{(A25)}$$

Solid-phase component balance for kth zone (kg/h)

(kg/h of component j = MeO)

$$\frac{d(W_R x_k^R)}{dt} = S_S x_k^S - S_R x_k^R - M_{MeS}(2/3)R_{O_2} \quad \text{(A26)}$$

Solid-phase component balance for kth zone (kg/h)

(kg/h of component j = inert)

$$\frac{d(W_R x_k^R)}{dt} = S_S x_k^S - S_R x_k^R \quad \text{(A27)}$$

Solid-phase energy balance for kth zone (kJ/h)

$$\frac{d(0.322W_R T^R)}{dt} = 0.322(S_S T^S - S_R T^R) + 36(F_{in}^R T_{in}^R - F_{out}^R T^R) - Q_R + \Delta H_{Rxn}R_{O_2} \quad \text{(A28)}$$

Kinetics

$$R_{O_2} = (3/2)R_{SO_2} = \mathrm{Conv}_R F^R_{in} y^R_{in,O_2} \quad \text{(A29)}$$

$$\mathrm{Conv}_R = 1 - \exp\left(-\frac{W_R K_R x^S_{R,MeS} y^R_{in,O_2}}{F^R_{in}}\right) \quad \text{(A30)}$$

where

$$K_R = K_{R0} \exp\left(-\frac{E_R}{(T_R + 273)R}\right) \quad \text{(A31)}$$

We used LSODE[40] to integrate the equations. The results obtained from our code were compared with those given by Luyben and Yi,[7,8] and there was a perfect match. For the complete model equations and FORTRAN code of the model, refer to Appendix C and G, respectively, of ref 39.

Nomenclature

B_d = health cost associated with each case of disease
b_j = binary variable = 0 if no experiments take place and =1 otherwise
$C_{lf,j}$ = fixed cost (for eg.example, the investment in a pilot plant for experimentation)
CH_4 = methane
CH_4^{in} = the moles of methane entering the fuel cell (kg·mol/hr)
CO^{in} = the moles of carbon monoxide entering the fuel cell (kg·mol/hr)
$\mathrm{Conv}_{S,k}$ = conversion at the kth zone in the desulfurizer
DRYCOA = mass inlet flowrate of dry coal to the power plant (lb/hr)
e^- = electron
Eff_k = ratio of actual conversion to ideal conversion at the kth zone
F = the Faraday constant (96 485 C/mol)
FC = per capita financial cost of program implementation
F^R_{in} = total molar flowrate of inlet gases to the regenerator (kg·mol/h)
F^R_{out} = total molar flowrate of outlet gases to the regenerator (kg·mol/h)
F^S_{in} = total molar flowrate of inlet gases to the desulfurizer (kg·mol/h)
F^S_{out} = total molar flowrate of outlet gases to the desulfurizer (kg·mol/h)
FUT = fuel utilization in SOFC
H_2 = hydrogen
H_2^{in} = the moles of hydrogen entering the cell (kg·mol/hr)
$H_2^{reacted}$ = the total moles of hydrogen reacted (kg·mol/hr)
H_2O = water
H_2S = hydrogen sulfide
HPPRES = pressure in HPSOFC (psi)
HPTEMP = temperature of high-pressure SOFC (°C)
I = the current (A)
i = the current density (mA/cm^2)
$K_{R,k}$ = reaction constant at the kth zone in the regenerator (kg·mol)(kg of sorbent)$^{-1}$h^{-1}
$K_{S,k}$ = reaction constant at the kth zone in the desulfurizer (kg·mol)(kg of sorbent)$^{-1}$h^{-1}
$-\ln(\sum \mathrm{varsamp}_{model})$ = proxy for time spent on researching fuel cell models
$-\ln(\sum \mathrm{varsamp}_{material})$ = proxy for time spent on researching fuel cell material
$-\ln(\sum \mathrm{varsamp}_{preexponential\ factor})$ = proxy for time spent on researching desulfurization reactions preexponential factors for different sorbents
$-\ln(\sum \mathrm{varsamp}_{activation\ energy})$ = proxy for time spent on researching desulfurization reactions activation energies for different sorbents
LPTEMP = temperature of low-pressure SOFC (°C)
m_k = the mean of the samples of the kth uncertain parameter
M^S_{in} = mean molecular weight of inlet gases to the desulfurizer (kg/kg·mol)
M^S_{out} = mean molecular weight of outlet gases to the desulfurizer (kg/kg·mol)
MeO = metal oxide
MeS = metal sulfide
MW_{GT} = power output of gas turbine module (MW)
MW_{ST} = output of steam turbine module (MW)
N = the number of samples of the kth uncertain parameter
$O^=$ = oxygen ion
O_2 = oxygen
O_2^{in} = the moles of oxygen entering the fuel cell (kg·mol/hr)
O_2^{out} = the moles of oxygen exiting the fuel cell (kg·mol/hr)
P_R = pressure in the regenerator (atm)
P_S = pressure in the desulfurizer (atm)
Q_R = heat removal from the regenerator (kJ/h)
$Q_{S,k}$ = heat removal from the kth zone in the desulfurizer (kJ/h)
$R_{j,k}$ = rate of reaction of component j in the desulfurizer (kg·mol/h)
RATIO = ratio of syngas routed to HPSOFC to that routed to LPSOFC
S_R = flowrate of solids from the regenerator (kg/h)
SO_2 = sulfur dioxide
SS_k = flowrate of solids from the kth zone in the desulfurizer (kg/h)
T_R = temperature in the regenerator (°C)
$T_{R,in}$ = temperature in the regenerator (°C)
$T_{S,k}$ = temperature at the kth zone in the desulfurizer (°C)
TRADC = temperature of syngas entering desulfurizer (°C)
$\mathrm{TSC}_{baseline}$ = total social cost for the baseline option (no testing for disease)
TSC_{option} = total social cost for the specified risk management option
U_f = the fuel utilization
V^S_G = gas volume in the desulfurizer (m^3)
$\mathrm{varsamp}_k$ = the sampling variance of the kth uncertain parameter
W_D = solid inventory in the drum (kg)
W_R = solid inventory in the regenerator (kg)
W_S = solid inventory in the desulfurizer (kg)
$W_{S,k}$ = solid inventory at the kth zone in the desulfurizer (kg)
$x_{i,k}$ = the ith sample of the kth uncertain parameter
$x_{k,j}{}^S$ = mole fraction of solid component j at the kth zone in the desulfurizer
$y_{k,j}{}^S$ = mole fraction of gas component j in the kth zone of the desulfurizer
$y_{in,j}{}^S$ = mole fraction of gas component j in the inlet gas of the desulfurizer
$y_{out,j}{}^S$ = mole fraction of gas component j in the outlet gas of the desulfurizer

Greek Letters

α = is a weight parameter

ϵ_j = new relative error level in the uncertain parameter θ_j after experimentation

ϵ_j^N = current nominal error level

Literature Cited

(1) National Energy Technology Laboratory (NETL). *Vision 21 Concept Plants: Fuel Cell/Gas Turbine Configuration 1*; U.S. Department of Energy: Morgantown, WV, 1998.

(2) Strakey, J. P. Vision 21: Advanced Power Plants for the 21st Century. Presented at the Advanced Coal-Based Power and Environmental Systems Conference, Morgantown, West Virginia, July 1998.

(3) http://www.netl.doe.gov/coalpower/vision21/

(4) Johnson, T. L.; Diwekar, U. M. Hanford Waste Blending and the Value of Research: Stochastic Optimization as a Policy Tool. *J. Multi-Criteria Decision Analysis* **2001**, *10*, 87−99.

(5) Johnson, T. L.; Diwekar, U. M. The Value of Design Research: Stochastic Optimization as a Policy Tool. In *Foundations of Computer-Aided Design*; Malone, M. F., Tainham, J. A., Carnahan, B., AIChE Symposium Series; American Institute of Chemical Engineers: New York, 2000; Vol. 96, pp 454−461.

(6) Diwekar, U. M. *Introduction to Applied Optimization*; Kluwer Academic Publishers: Dordrecht, The Netherlands, 2003.

(7) Luyben, W.; Yi, C. K. Dynamic modeling and control of a hot-gas desulfurization process with a transport desulfurizer. *Ind. Eng. Chem. Res.* **2001**, 40, 1157−1167.

(8) Luyben, W.; Yi, C. K. Dynamic model and control structure of a hot gas desulfurization fluidization process. *Ind. Eng. Chem. Res.* **1999**, *38*, 4290−4298.

(9) National Energy Technology Laboratory (NETL). *Fuel cell handbook*, fifth ed.; U.S. Department of Energy: Morgantown, WV, 2000.

(10) AspenTech. *Aspen Plus Documentation*, Version 12.1; AspenTech: Cambridge, MA, 2003.

(11) Geisbrecht, R. Compact Electrochemical Reformer Based on SOFC Technology. Presented at AIChE Spring National Meeting, Atlanta, GA, 2000.

(12) Petruzzi, L.; Cocchi, S.; Fineschi, F. A global thermo-electrochemical model for SOFC systems design and engineering. *J. Power Sources* **2003**, *118*, 96−107.

(13) Aguiar, P.; Chadwick, D.; Kershenbaum, L. Modeling of an indirect internal reforming solid oxide fuel cell. *Chem. Eng. Sci.* **2002**, *57*, 1665−1677.

(14) Campanari, S. Thermodynamic model and parametric analysis of a tubular SOFC module. *J. Power Sources* **2001**, *92*, 26−34.

(15) Chan, S. H.; Khor, K. A.; Xia, Z. T. A Complete Polarization Model of a Solid Oxide Fuel Cell and its Sensitivity to the Change of Cell Component Thickness. *J. Power Sources* **2001**, *93*, 130−140.

(16) Cownden, R.; Nahon, M.; Rosen, M. A. Modeling and analysis of a solid polymer fuel cell system for transportation applications. *Int. J. Hydrogen Energy* **2001**, *26*, 615−623.

(17) Nagata, S.; Momma, A.; Kato, T.; Kasuga, Y. Numerical analysis of output characteristics of tubular SOFC with internal reformer. *J. Power Sources* **2001**, *101*, 60−71.

(18) Xui-Mei, G.; Hidajat, K.; Ching, C. Simulation of a solid oxide fuel cell for oxidative coupling of methane. *Catal. Today* **1999**, *50*, 109−116.

(19) Virkar, A. V.; Chen, J.; Tannel, C. W.; Kim, J. The role of electrode microstructure on activation and concentration polarizations in solid oxide fuel cells. *Solid State Ionics* **2000**, *131*, 189−198.

(20) Al-Qattan, A. M.; Chmielewski, D. J.; Al-Hallj, S.; Selman, J. R. A novel design for solid oxide fuel cell stacks. *Chem. Eng. Sci.* **2004**, *59*, 131−137.

(21) Chachuat, B.; Mitsos, A.; Barton, P. I. Optimal design and steady-state operation of micro power generation employing fuel cells. *Chem. Eng. Sci.* **2005**, *60*, 4535−4556.

(22) Padulles, J.; Ault, G. W.; McDonald, J. R. An integrated SOFC plant dynamic model for power systems simulation. *J. Power Sources* **2000**, *86*, 495−500.

(23) Urban, Z.; Pantelides, C. C. High accuracy predictive modeling of for solid oxide fuel cell units in systems. *Proceedings of the Eighth Grove Fuel Cell Symposium*, London, U.K., 2003.

(24) Hall, D. J.; Colclaser, R. G. Transient Modeling and Simulation of a Tubular Solid Oxide Fuel Cell. *IEEE Trans. Energy Convers.* **1999**, *14*, 749−753.

(25) Baratto, F. Impacts assessment and tradeoffs of fuel cell based auxiliary power units. Master's thesis, University of Illinois at Chicago, Chicago, IL, 2004.

(26) Arthur, D. L. Inc. *Conceptual Design of POX/SOFC 5kW Net System*; Final report to Department of Energy; National Energy Technology Laboratory, U.S. Department of Energy: Morgantown, WV, 2001.

(27) Subramanyan, K.; Diwekar, U. Characterization and quantification of uncertainty in solid oxide fuel cell hybrid power plants. *J. Power Sources* **2005**, *142*, 103−116.

(28) Bernardo, P. F.; Saraiva, P. M.; Pistikopoulous, E. N. Inclusion of information costs in process design optimization under uncertainty. *Comput. Chem. Eng.* **2000**, *24*, 1695−1701.

(29) Bartell, S. M.; Ponce, A. R.; Takaro, K. T.; Zerbe, O. R.; Omenn, G. S.; Faustman, E. M. Risk estimation and value-of-information analysis for three proposed genetic screening programs for chronic beryllium disease prevention. *Risk Anal.* **2000**, *1*, 87−99.

(30) Casimir, R. J. The value of information in the multi-item newsboy problem. *Omega* **2002**, *30*, 45−50.

(31) Nadiminti, R.; Mukhopadhyay, T.; Kriebel, C. H. Risk aversion and the value of information. *Decision Support Syst.* **1996**, *16*, 241−254.

(32) Meltzer, D. Addressing uncertainty in medical cost-effectiveness analysis: Implications of expected utility maximization for methods to perform sensitivity analysis and the use of cost-effectiveness analysis to set priorities for medical research. *J. Health Economics* **2001**, *20*, 109−129.

(33) Krieger, D. J.; Hoehn, J. P. The economic value of reducing environmental health risks: contingent valuation estimates of the value of information. *J. Environ. Manage.* **1999**, *56*, 25−34.

(34) Ramer, A.; Padet, C. Information semantics of possibilistic uncertainty. *Fuzzy Sets Syst.* **1995**, *69*, 299−303.

(35) Varis, O. Bayesian decision analysis for environmental and resource management. *Environ. Modell. Software* **1997**, *2−3*, 177−185.

(36) Gokcay, K.; Bilgic, T. Troubleshooting using probabilistic networks and value of information. *Int. J. Approximate Reasoning* **2002**, *29*, 107−133.

(37) Linville, C. D.; Hobbs, B. F.; Venkatesh, B. N. Estimation of error and bias in Bayesian Monte Carlo decision analysis using the bootstrap. *Risk Anal.* **2001**, *1*, 63−74.

(38) Gottinger, H. W.; Hans, W. Choosing regulatory options when environmental costs are uncertain. *Eur. J. Operational Res.* **1996**, *88*, 28−37.

(39) Subramanyan, K. Multi-objective optimization of hybrid fuel cell power systems under uncertainty and the "value of research". Master's thesis, University of Illinois at Chicago, Chicago, IL, 2004.

(40) Radhakrishnan, K.; Hindmarsh, A. C. *Description and use of LSODE, the Livermore Solver for Ordinary Differential Equations*; Lawrence Livermore National Laboratory Report UCRL-ID-113855; Lawrence Livermore National Laboratory: Livermore, CA, 1993.

Received for review August 24, 2004
Revised manuscript received October 26, 2005
Accepted November 2, 2005

IE0492247